

Toughness-Temperature Curves in Oxide Dispersion Strengthened MA957- M.J. Alinger, G.R. Odette and G.E. Lucas (University of California, Santa Barbara)

OBJECTIVE

The objective of this work is to assess the fracture toughness as a function of test temperature and crack orientation in oxide dispersion strengthened (ODS) MA957 as a baseline for developing high performance nano-composited ferritic alloys.

SUMMARY

Iron based alloys strengthened with a very high density and fine dispersion of ultra-fine scale yttria-titanium-oxygen particles for improved high temperature creep strength, coupled with chromium additions for corrosion resistance, offer great promise for elevated temperature applications in fusion reactors. These alloys are usually referred to as oxide dispersion strengthened (ODS) steels. They are typically produced through mechanical alloying by mixed powder attrition, followed by consolidation and hot deformation, which may include the production of near net shape components. Given their engineered microstructural architectures and low carbon content (a key factor in their success), we feel it is more appropriate to refer to this class of materials as nano-composited ferritic alloys (NFAs).

Mechanically alloyed 14Cr-1Ti-0.3Mo-0.025Y₂O₃ MA957 in the form of extrusions, were produced and extensively characterized for the breeder reactor program [1]. This material showed very promising creep and tensile properties. However, limited Charpy testing demonstrated that this MA957 product has highly anisotropic grain structures and manifests extremely brittle behavior, particularly in certain orientations. Brittle behavior was attributed to the presence of alumina stringers. The objective of the present work is to characterize the fracture toughness-temperature curves for MA957 in various orientations relative to the grain and inclusion structures. Small, pre-cracked, 1/3-sized Charpy specimens of MA957 tested in three point bending under quasi-static conditions showed low minimum toughness (<20MPa√m) and lower transition cleavage up to temperatures around 50-70°C in both the C-R and C-L orientations. At higher temperatures these orientations also manifested low resistance to stable crack growth, with maximum load toughness values ranging from about 50-100 MPa√m. However, the cleavage regime is shifted to much lower temperatures of around -70°C for the L-R orientation; and at high temperature maximum load toughness increased to about 125 to 145 MPa√m. At intermediate temperatures the fracture process was complex, typically involving out of plane cracking and combinations of stable extension and small cleavage pop-in events. The latter results are very encouraging and suggest that with proper development, NFA systems offer great promise to combine very high strength with good toughness and corrosion resistance.

PROGRESS AND STATUS

Introduction

Ferritic and martensitic steels are attractive candidates for structural applications in fusion reactors owing to their resistance to swelling under irradiation and inherent low activation character. Unfortunately, the creep resistance of steels such as F82H is insufficient for temperatures above about 600°C. However, the creep strength of ferritic (and other metal based) systems can be greatly increased by mechanical alloying (MA) iron and chromium powders with fine scale dispersants [Y(Ti)₂O₃]. The MA powders can then be consolidated, hot deformed and thermally treated by a variety of methods to yield desired product forms. Recently it has been observed that MA and consolidation of ferritic powders with Y₂O₃ and Ti can produce ultra fine, nm-scale, coherent Y-O-Ti clusters, as well as more typical fine-to-coarser scale incoherent

Y(Ti)₂O₃ dispersed oxide particles [2]. The processing route and engineered reinforcement architecture produce what we call nano-composited ferritic alloys (NFAs). A current challenge to studying NFAs is that they are not currently commercially available, and generally exist only in small laboratory batch-sized quantities that are restricted in use. An exception is patented (U.S. Patent 4,075,010 [3]) MA957. Several forms of MA957 were procured for characterization of their basic mechanical properties in the 1980s by the US Breeder Reactor Alloy Development Program [1]. However, data on the fracture resistance of MA957 is limited to a small number of Charpy V-notch tests. Fortunately, though the efforts of Dr. D. Gelles of Pacific Northwest National Laboratory (PNNL), a residual stock of MA957 has been located, and he has supplied material to UCSB in the form of approximately 103 mm of a 25 mm diameter extrusion. This MA957 product is being used to develop a baseline understanding of the performance of NFAs, with initial emphasis on fracture toughness.

Indeed, low toughness is a potential problem with NFAs, since in common with other BCC metals and alloys, they exhibit a transition from 'ductile' stable crack growth to brittle cleavage fracture in a characteristic low temperature regime. Further, the very high strength (the yield stress for MA957 used in this study is more than 1100 MPa at room temperature) would be expected to decrease toughness relative to conventional steels. In addition, during extrusion processing the MA957 (and similar alloys) develop highly anisotropic grain structures and corresponding variations in properties with specimen orientation. Moreover, MA processing routes are vulnerable to impurity contamination. Unfortunately, the current MA957 product was contaminated with alumina (Al₂O₃) stringers deriving from impurities in the ferrochrome powder used to supply the chromium to the alloy [1]. These stringers are extremely detrimental to the mechanical properties of this MA957 product.

The objective of the current study is to characterize the toughness-temperature behavior of the MA957 product as a function of specimen orientation. Coupled with other measurements, which are in progress, these data will provide insight on the fracture mechanisms in this material system as well as guidance regarding approaches to improving the performance and ultimate potential of NFAs in general.

Experiment

The MA957 was procured from PNNL in the form of a hot-extruded bar produced by International Nickel Company (INCO). The chemical composition is shown in Table 1, and details of the processing can be found in Reference 1.

Table 1. Nominal Chemical Composition of MA957 (wt%)

	Cr	Ti	Mo	Y ₂ O ₃	Fe
MA957	14.0	1.0	0.3	0.25	Bal.

Previous microstructure characterization showed highly anisotropic structures with equiaxed grains in the transverse direction ($\approx 0.5\mu\text{m}$) but with significant elongation in the longitudinal direction resulting in a $\approx 10:1$ aspect ratio; alumina stringers aligned in the longitudinal direction were also observed [1].

Small, 1/3-sized Charpy specimens (3.33 x 3.33 x 25.4 mm) were electro-discharge machined from the as-received bar in three orientations with respect to the extrusion direction as shown in Figure 1. Per ASTM Standard E399, these orientations included: a) circumferential specimen length-longitudinal crack plane (C-L); b) circumferential specimen length-radial crack plane (C-R); and c) longitudinal specimen length-radial crack plane (L-R). Micro-hardness measurements

($\approx 355 \text{ kg/mm}^2$) revealed little variation in strength through the cross-section of the bar. Fatigue pre-cracking was carried out at a final $\Delta K \leq 15 \text{ MPa}\sqrt{\text{m}}$ to a nominal crack length (a) to specimen width (W) ratio $a/W = 0.5$.

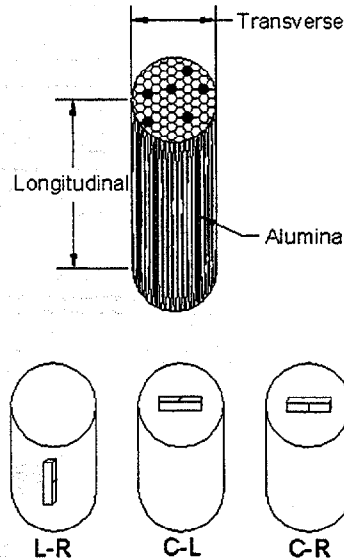


Figure 1. Specimen orientation showing grain anisotropy and alumina (Al_2O_3) stringers.

The specimens were tested in three point bending over a temperature range from -196 to 150°C at approximate loading rates of $2.5 \times 10^{-6} \text{ m/s}$ in accordance with testing guidelines in ASTM Standard E1921-97 [4]. Load and load line displacement were monitored during testing. Depending on specimen orientation and temperature, the failure event was either a result of unstable cleavage crack propagation, cleavage pop-ins and unstable crack tearing or some combination of these. In all cases, K_{Jc} was determined from: $K_{Jc} = (E'J_{1c})^{1/2}$, where E' is the plane strain elastic modulus and J_{1c} is the elastic-plastic energy release rate determined from the elastic stress intensity and the compliance corrected area under the stress-displacement curve up to the fracture or pop-in load drop per ASTM 1921-97. In several cases, a maximum load was exhibited without a pop-in event. In these cases, an effective maximum load toughness, K_m , was determined from the stress-displacement curve. The high yield stress (σ_y) resulted in sufficient (although not totally full) constraint up to K_{Jc} values near the ASTM 1921-97 censoring criteria for cleavage nucleation of $\sigma_y E' b / K_{Jc}^2 > 30$. Note that cases with extensive stable crack growth and complex fracture path are not technically 'valid' but nevertheless represent useful measures of effective toughness.

Results

Figures 2-4 summarize the $K_{Jc/m}$ versus temperature data for the specimens tested in three orientations. The filled triangles indicate linear elastic cleavage fracture. The filled circles indicate elastic-plastic cleavage, including cases where some stable crack growth was mixed with pop-ins. The filled diamonds correspond to K_m , where some form of stable crack growth was exhibited along with minimal pop-ins. It is evident that the toughness and the cleavage transition temperature regime are highly dependent on orientation. These large toughness variations are believed to be due to the alumina stringers and anisotropic grains.

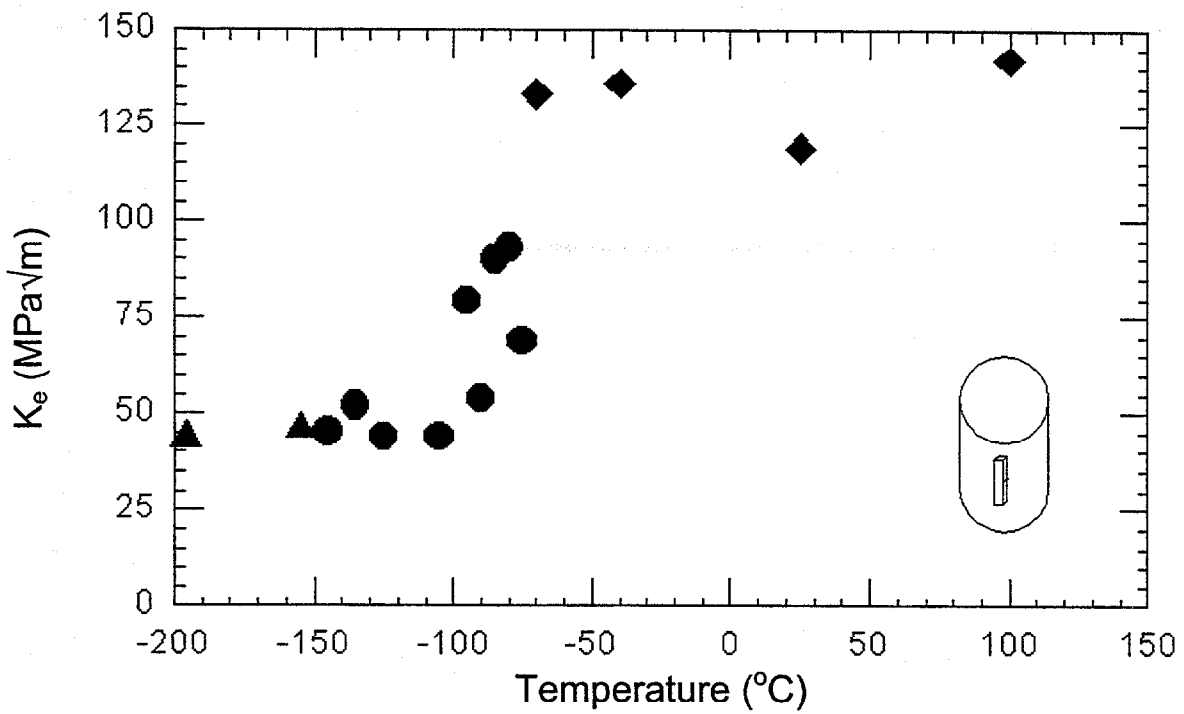


Figure 2. K_e Vs. Temperature for L-R orientation.

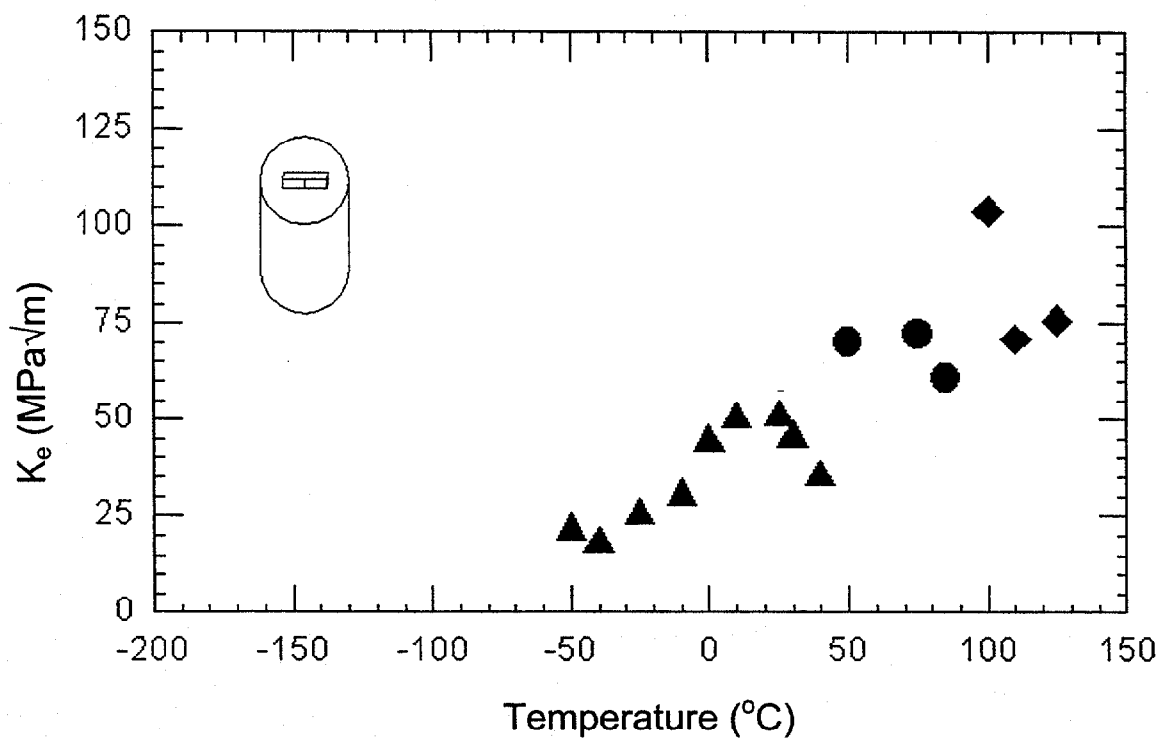


Figure 3. K_e Vs. Temperature curve for C-R orientation.

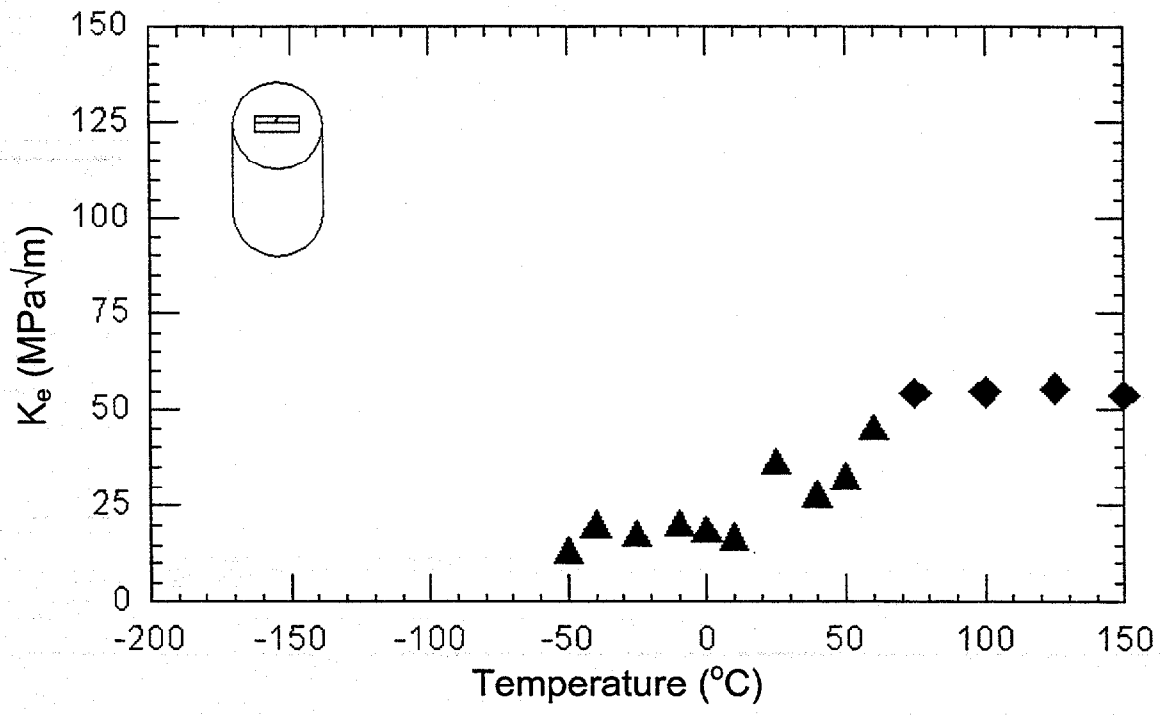


Figure 4. K_e Vs. Temperature for C-L orientation.

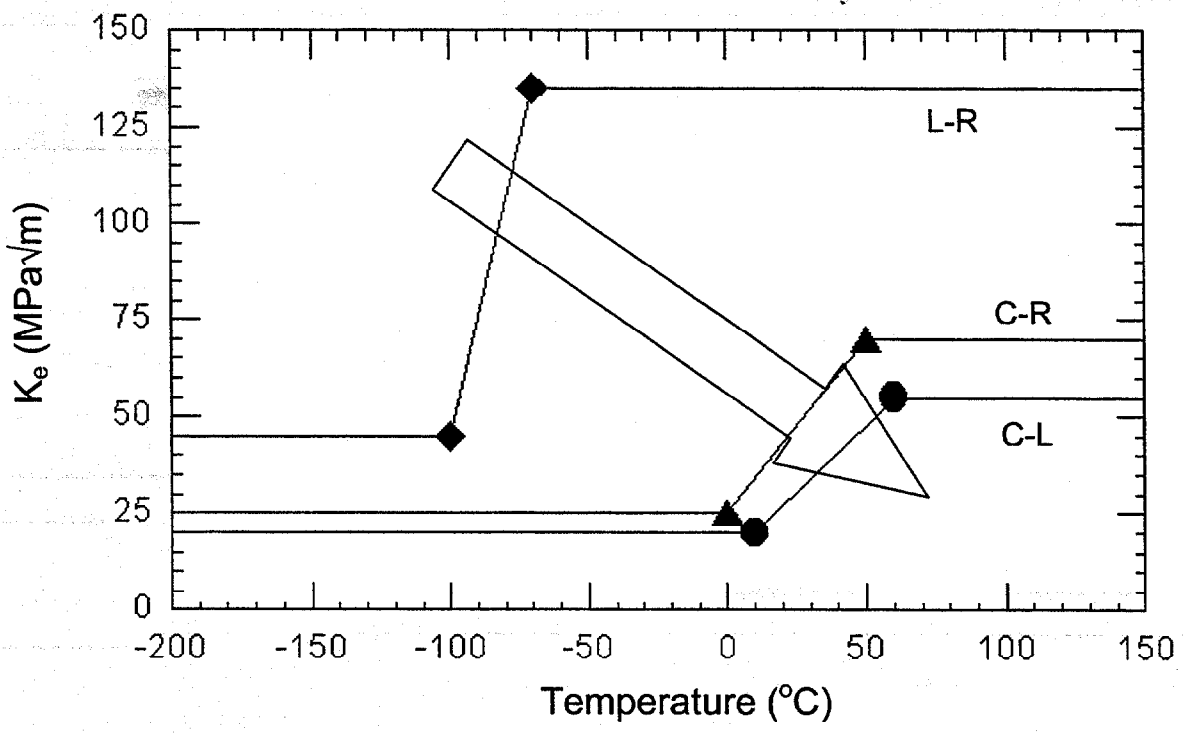


Figure 5. K_e Vs Temperature Summary for All Orientations.

As shown in Figure 2, the L-R orientation exhibits the highest toughness levels and the lowest cleavage transition temperature range. The transition to stable crack growth occurs at about -70°C . However, even at much lower temperatures (down to about -145°C) fracture occurs by a series of small pop-ins between arrest events with what appears to be a minimum of intervening stable growth.

The toughness levels for both circumferential orientations are much lower. Figure 3 shows the results for the C-R orientation, with intermediate toughness. Below about 50°C fracture is linear elastic with $K_{Ic} < 60 \text{ MPa}\sqrt{\text{m}}$. Between 70 and 100°C there is some plasticity prior to cleavage, but the toughness remains low with $K_{Ic} \leq 75 \text{ MPa}\sqrt{\text{m}}$. Ductile tearing occurs above about 100°C at about $75 \text{ MPa}\sqrt{\text{m}}$. Note, the $K_m \approx 110 \text{ MPa}\sqrt{\text{m}}$ point is misleading since crack tearing starts below general yield in this case.

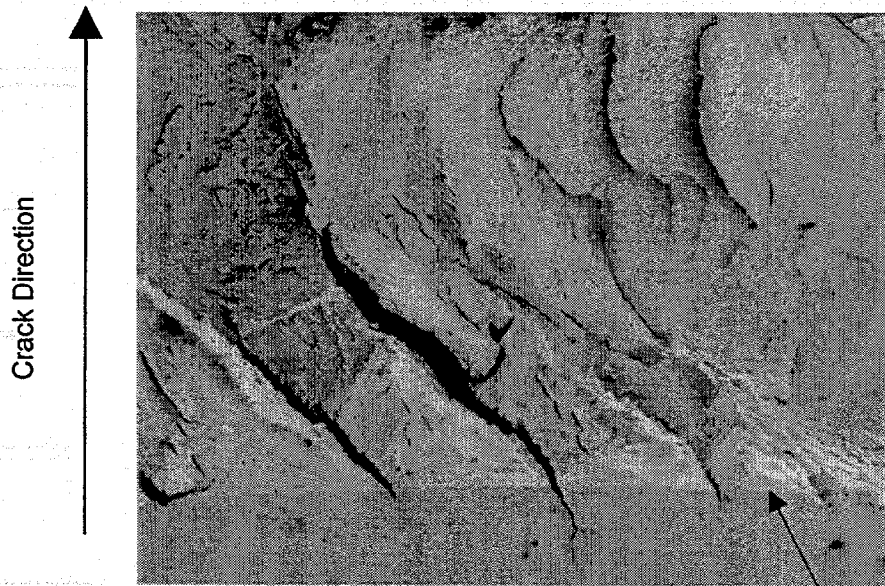
Figure 4 shows results for the C-L orientation, which has the lowest toughness. While the toughness increases with temperature, fracture is linear elastic up to 50°C and has only a very small amount of plasticity up to 75°C . Above 100°C it appears that stable crack tearing occurs close to or even before general yield at a very low $K_m (=K_{Ic})$ of about $60 \text{ MPa}\sqrt{\text{m}}$. The magnitude of the upper and lower shelves decrease as well to about $20 \text{ MPa}\sqrt{\text{m}}$ and $55 \text{ MPa}\sqrt{\text{m}}$, respectively.

DISCUSSION

Figure 5 summarizes the effect of specimen orientation on the transition temperature range as well as the respective calculated effective toughnesses. The fracture toughness trends reflect the high degree of microstructural anisotropy and the deleterious effects of the alumina stringers on cleavage fracture. The highest toughness occurred when the crack grew across the short dimension of the elongated grains and orthogonal to the alumina stringers, thereby intersecting the smallest cross section area of the inclusions. The lowest toughness occurred when crack growth was along the longitudinal direction, parallel to the long dimension of the grains and the quasi-continuous length of the inclusions. Intermediate behavior occurred when the inclusion stringers ran parallel to the crack front. This suggests that cleavage fracture is promoted by crack growth in directions of large grain dimension and by a high density in the crack path of alumina inclusions, which act as trigger particles for cleavage.

These conclusions are supported by SEM Fractography shown in Figures 6 to 11. Cracking in the L-R orientation is primarily out-of-plane, transverse to the fracture surface, which shows what appear to be substantial levels of deformation (Figures 6 and 7). The fracture in the C-R orientation also has transverse components and a somewhat torturous path with ductile dimples mixed with cleavage facets on the surface (Figures 8 and 9). In contrast, the C-L orientation shows a very flat fracture surface with only limited indications of ductile fracture, split inclusions and a minimal difference between the pre-crack and predominantly cleavage surface (Figures 10 and 11). These detailed examinations are continuing and will be described in future reports.

Clearly, the generally low, and highly orientation-dependent toughness of this MA957 product do not provide acceptable levels of performance for fusion applications. However, the results in the C-R and C-L orientation are important primarily for fundamental reasons. The much better results for the L-R orientation are more technologically important, since they probe conditions of crack growth in the direction of small grain dimension and of minimum density in the crack path of impurity inclusions that act as the trigger particles for cleavage. These results indicate that removal of the brittle alumina stringers as well as a reduction in the 10:1 aspect ratio of the grain morphology will likely provide a material with both good toughness and very high strength as well as good corrosion resistance.



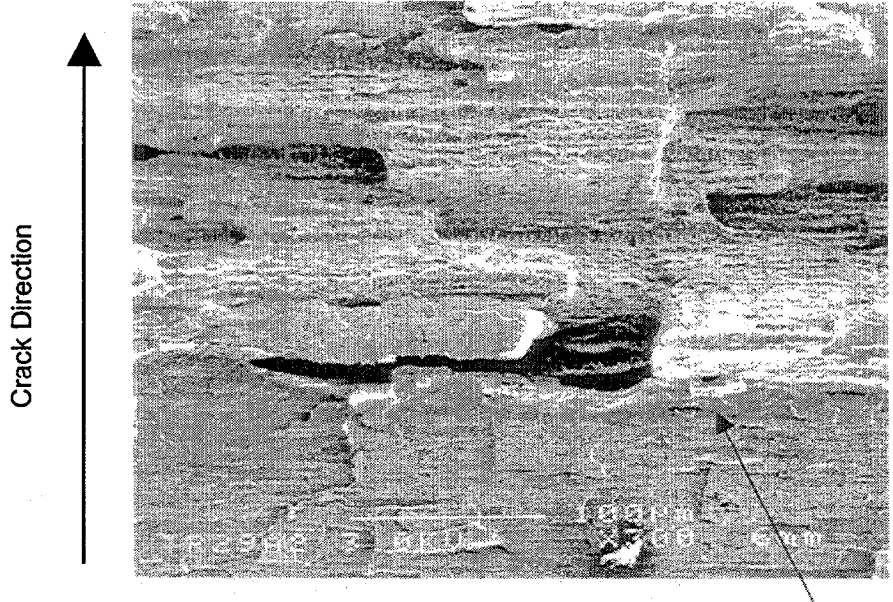
Pre-Crack

Figure 6. SEM image of fracture surface in L-R orientation tested at -80°C .



Pre-Crack

Figure 7. SEM image of fracture surface in L-R orientation tested at -70°C .



Pre-Crack

Figure 8. SEM image of fracture surface in C-R orientation tested at -40°C .

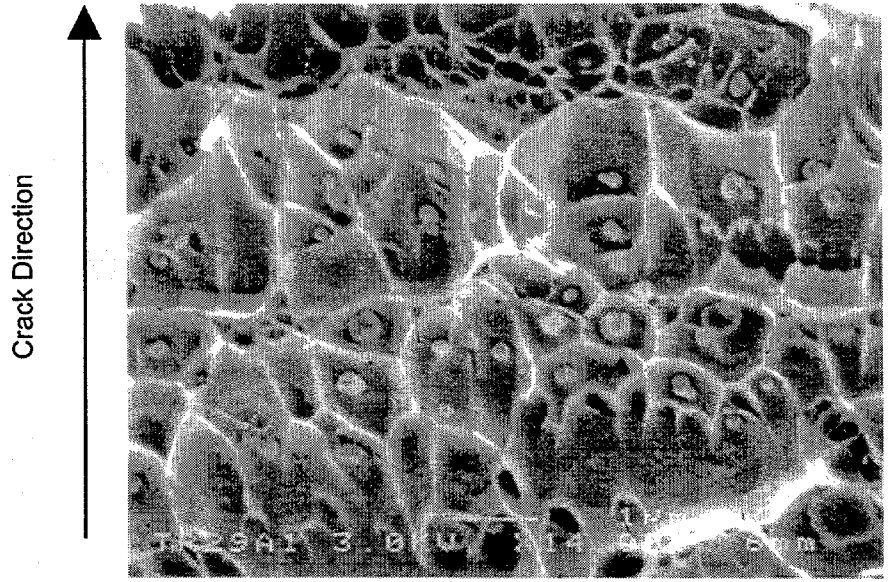


Figure 9. SEM image of fracture surface in C-R orientation tested at -80°C .



Figure 10. SEM image of fracture surface in C-L orientation tested at 25°C.

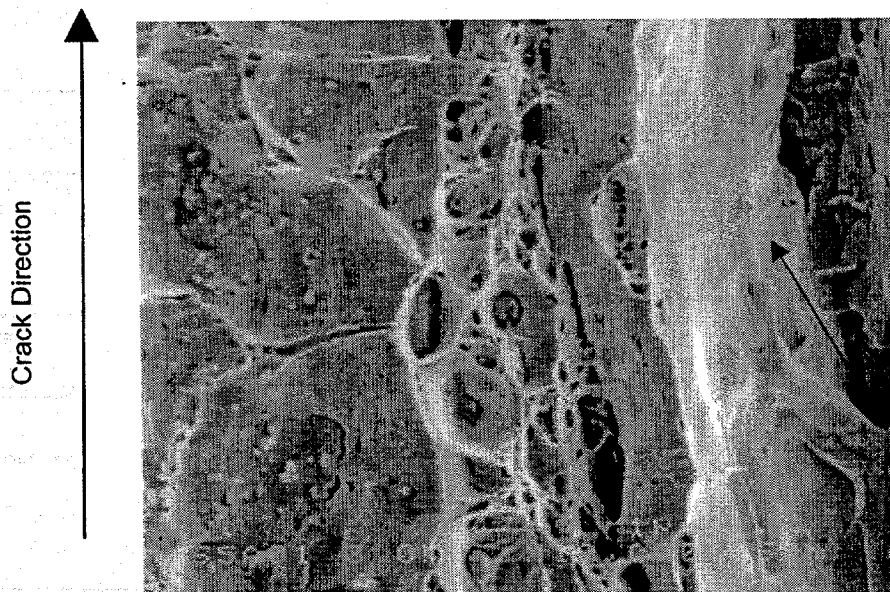


Figure 11. SEM image of fracture surface in C-L orientation tested at 25°C.

FUTURE WORK

Investigation of some details of fracture of the MA957 product examined in this study will continue with emphasis on high resolution Fractography to characterize the mix of fracture mechanisms and to identify crack nucleation sites and the role of inclusions in crack propagation. However, given the very promising results for the L-R orientation, efforts will be initiated to procure some new high purity and more isotropic NFAs in the MA957 class with the intention of baselining what is expected to be their superior toughness performance. Further optimizations of the balance of properties using a materials system design approach will follow.

ACKNOWLEDGMENTS

This work was supported in part by the Office of Fusion Energy, DOE, Grant No. DE-FG03-87ER-52143.

REFERENCES

1. Hamilton, M.L. *et al*, "Fabrication Technological Development of the Oxide Dispersion Strengthened Alloy MA957 for Fast Reactor Applications", PNNL-13168, PNL, Richland, WA, 2000.
2. Okuda, T. and M. Fujiwara, "Dispersion Behaviour of Oxide Particles in Mechanically Alloyed ODS Steel", *Journal of Materials Science Letters*, V14, pp 1600-1603, 1995.
3. Fischer, J.J., U.S. Patent 4,075,010, "Dispersion Strengthened Ferritic Alloy for use in Liquid Metal Fast Breeder Reactors", issued Feb. 21, 1978.
4. E 1921-97, "Standard Test Method for Determination of Reference Temperature, T_0 , for Ferritic Steels in the Transition Range", American Society for Testing and Materials, Philadelphia, 1997.